Supporting Information for

Improving the long-term weatherability of commercial radiative cooling materials by a fluorine-free superhydrophobic coating

Ze-Ye Wang[a,b]‡, Xian Wu[a,b]‡, Ming-Liang Qu[a,b], Zi-Rui Li[a,b], Guang-Yan Zhou[a,b], Yi-Chao Wang[c], Hui Liu[c], Jiang Lu[d], Zi-Tao Yu[a,b], Li-Wu Fan[a,b,*1]

[a]*State Key Laboratory of Clean Energy Utilization, Zhejiang University, Hangzhou, Zhejiang 310027, People's Republic of China*

[b]*Institute of Thermal Science and Power Systems, College of Energy Engineering, Zhejiang University, Hangzhou, Zhejiang 310027, People's Republic of China*

[c]*ZheJiang Province Erjian Construction Group Co.,Ltd., Ningbo, Zhejiang 315000, People's Republic of China*

[d] *School of Civil Engineering and Architecture, Zhejiang University of Science and Technology, Hangzhou, 310023, People's Republic of China*

*Corresponding author. Tel./fax: +86 571 87952378 (L.-W. Fan).

E-mail address: liwufan@zju.edu.cn (L.-W. Fan).

‡These two authors contributed equally to this article.

S1 Commercial RC materials characterization

We characterized the microstructure and roughness of commercial RC materials.

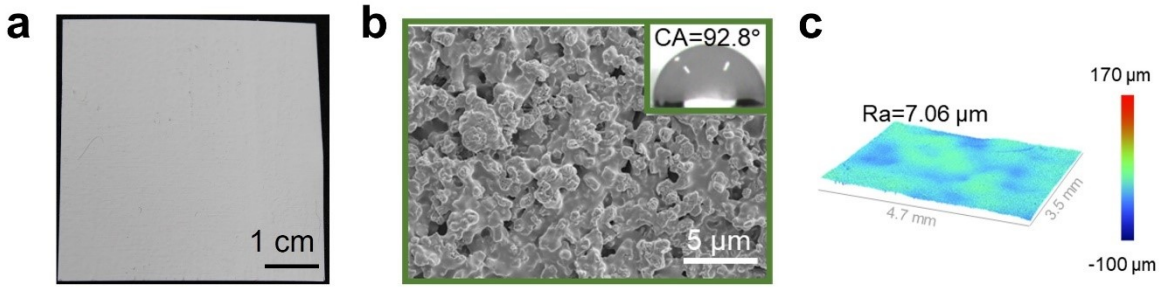

Fig S1. (a) Photo. (b) SEM image. (c) The surface roughness.

S2 PDMS curing procedure

In this study, the FTIR testing of PDMS was conducted on the cured PDMS, with the specific steps as follows: Firstly, 15 g of the PDMS base component were mixed with 1.5 g of curing agent in a 10:1 ratio. To ensure the mixture was homogeneous, it was stirred using a magnetic stirrer for 1 h. Subsequently, the mixture was left to stand at room temperature for 1 h to allow all internal bubbles to fully dissipate. Finally, the degassed PDMS mixture was placed in an oven and cured at 80 °C for one hour to complete the curing process.

S3 Determination of the content and ratio of dual-scale SiO_2

To achieve optimal superhydrophobic surface performance, various micro/nano hierarchical surfaces were prepared. Firstly, by testing the static contact angle at a μ-SiO_2:n-SiO_2 ratio of 1:1, it was found that when μ-SiO_2 and n-SiO_2 were each 0.65 g, the CA reached a favorable value of 158.2°. Subsequently, with the total mass of μ-SiO_2 + n-SiO_2 fixed at 1.3 g, the CA was further investigated under different SiO_2 ratios. The results indicated that the better performance was achieved at a μ-SiO_2: n-SiO_2 ratio of 1:1. Ultimately, the composition was determined to be 0.65 g each of μ-SiO_2 and n-SiO_2.

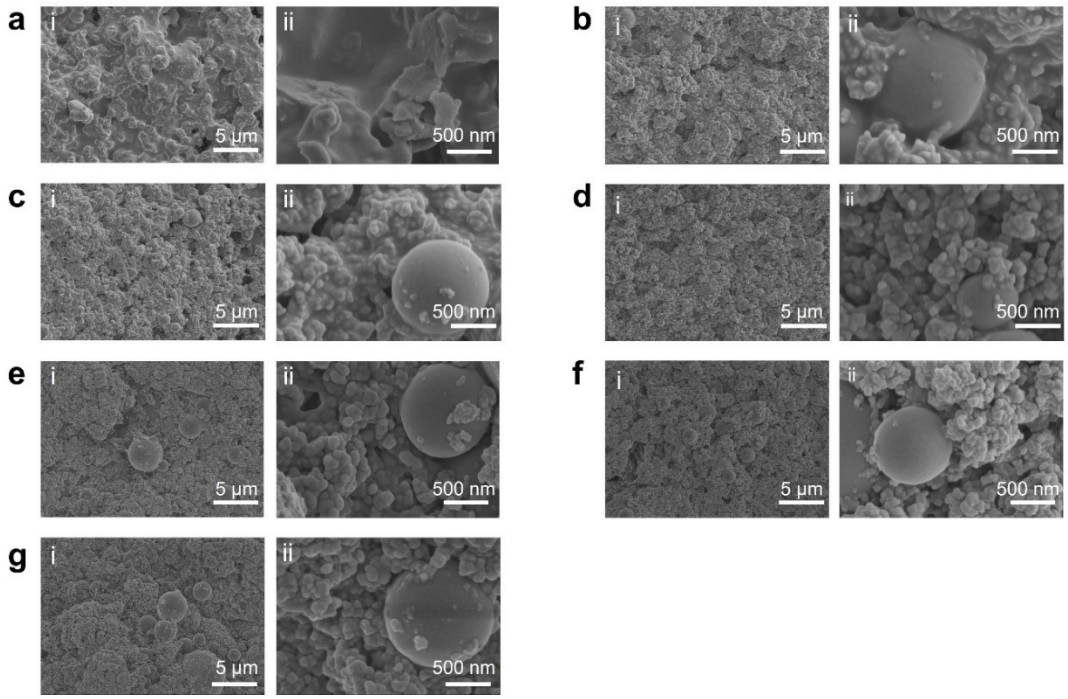

Fig S2. SEM images of superhydrophobic coatings sprayed onto commercial RC with different masses μ-SiO_2 and n-SiO_2. (a) μ-SiO_2= n-SiO_2=0.1 g; (b) μ-SiO_2= n-SiO_2=0.2 g; (c) μ-SiO_2= n-SiO_2=0.3 g; (d) μ-SiO_2= n-SiO_2=0.4 g; (e) μ-SiO_2= n-SiO_2=0.5 g; (f) μ-SiO_2= n-SiO_2=0.6 g; (g) μ-SiO_2= n-SiO_2=0.7 g

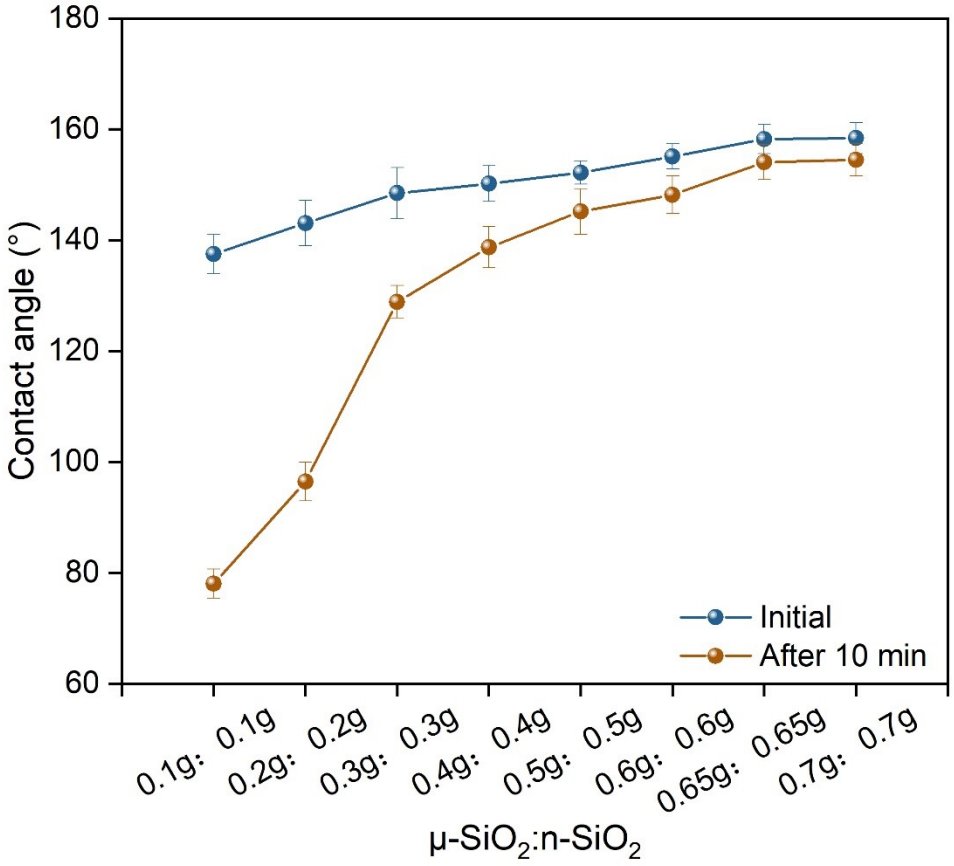

Fig S3. CAs of superhydrophobic coating with different SiO_2 contents

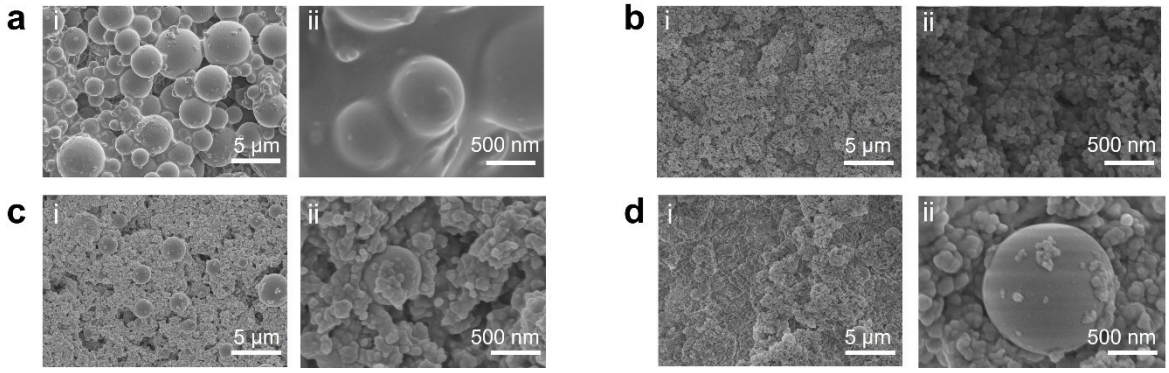

Fig S4. SEM images of superhydrophobic coatings sprayed onto commercial RC with different ratios μ-SiO_2 and n-SiO_2 (μ-SiO_2 + n-SiO_2 =1.3 g). (a) μ:n=1:0; (b) μ:n=0:1; (c) μ:n=2:1, (d) μ:n=1:2

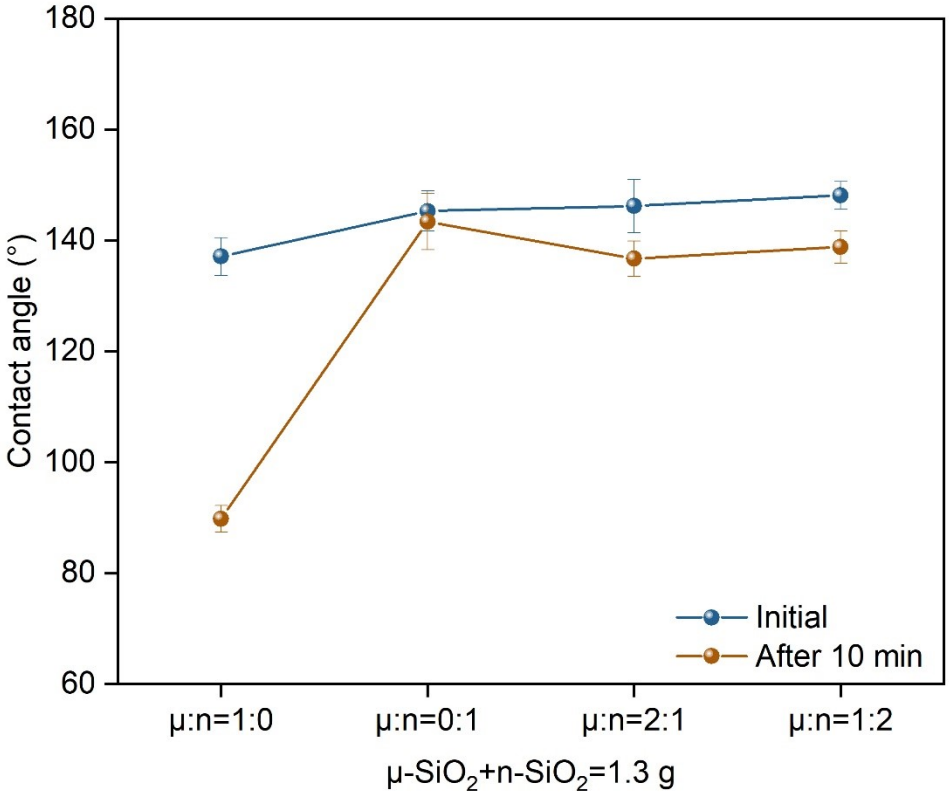

Fig S5. CAs of superhydrophobic coating with different SiO_2 ratio

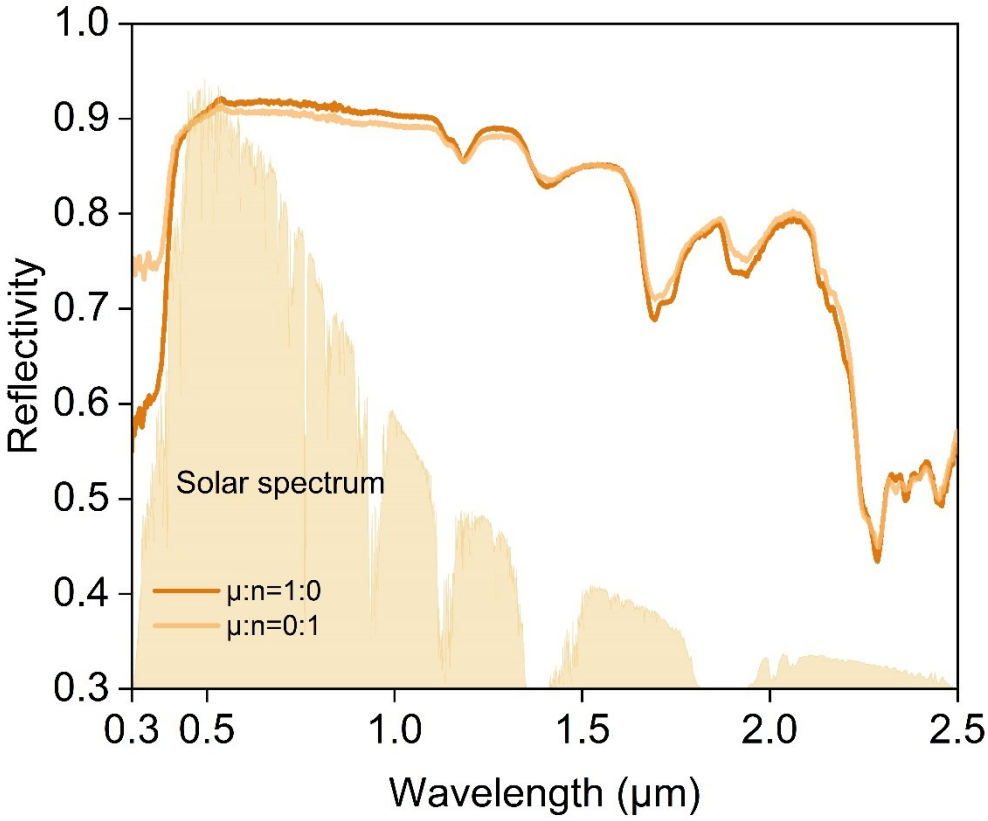

Fig S6. Reflectivity of commercial RC with different SiO_2 ratio superhydrophobic coating

We fabricated superhydrophobic coatings with different thicknesses on the surface of commercial RC materials by controlling the spraying time, in order to investigate the influence of coating thickness on the original radiative performance. The coating thickness was measured using a laser-based thickness gauge. We tested samples with coating thicknesses of ~20 μm, ~80 μm, and ~100 μm, which exhibited solar reflectivity values of 0.87, 0.89, and 0.89, respectively. In the main experiments, a coating thickness of ~50 μm was used, which also showed a reflectivity of 0.89. These results indicate that variations in coating thickness within a reasonable range do not significantly affect the solar reflectivity of the coated RC surface.

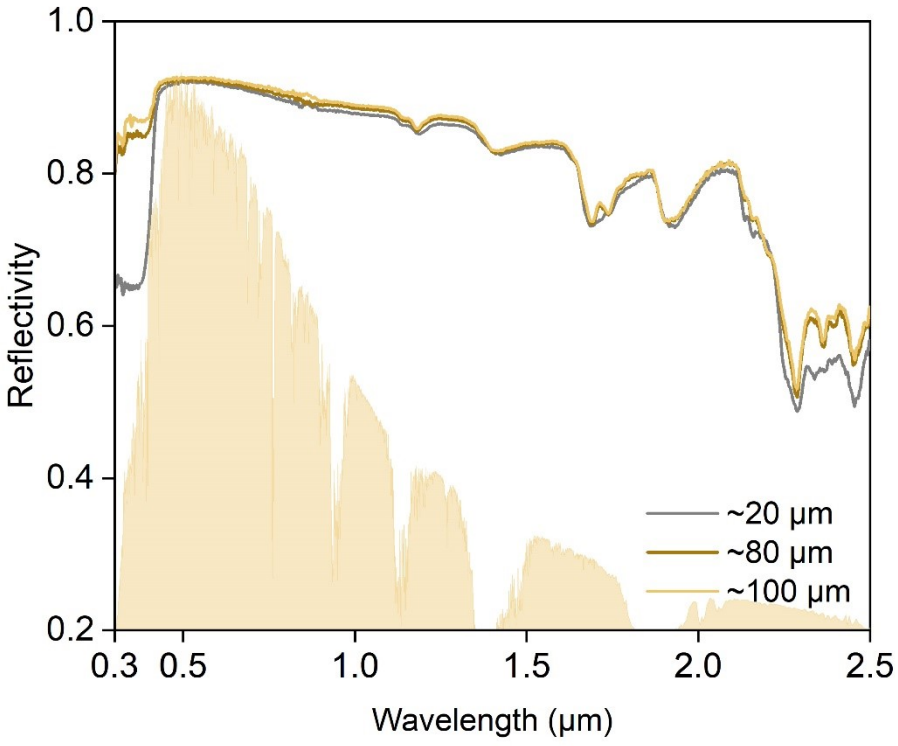

Fig S7. Reflectivity of superhydrophobic RC with different thicknesses of superhydrophobic coatings

S4 Outdoor RC performance measurements

To investigate the cooling effects, a custom-built experimental setup was employed. A figure of this setup is shown in Figure 2a. The interior of the device was filled with thermal insulation cotton to ensure proper insulation. Commercial RC and superhydrophobic RC were placed tightly on the top of the setup, and the sides were covered with aluminum foil to minimize external radiation absorption. PT100 temperature probes (accuracy 0.1 ℃) were installed on the back of the samples, and transient temperature data were recorded using a data logger (TH2553, accuracy 0.1 ℃). The setup was positioned one meter above the ground to reduce convective heat exchange with the ground. Meteorological parameters such as solar irradiance, wind speed, and humidity were collected using an automatic weather station (Jinzhou Sunshine Meteorological Technology Co., Ltd.), and rainfall data were collected using a rain gauge (Weihai Jingxun Changtong Electronic Technology Co., Ltd.). Figure S8 shows the meteorological data at the test stand location during the test period. The data gap occurring between 16:00 on 1 August 2024 and 12:50 on 19 August 2024 was attributed to equipment failure in the automated weather station system. Missing meteorological parameters during this period were supplemented using commercially available datasets from the Xihe Energy Big Data Platform.

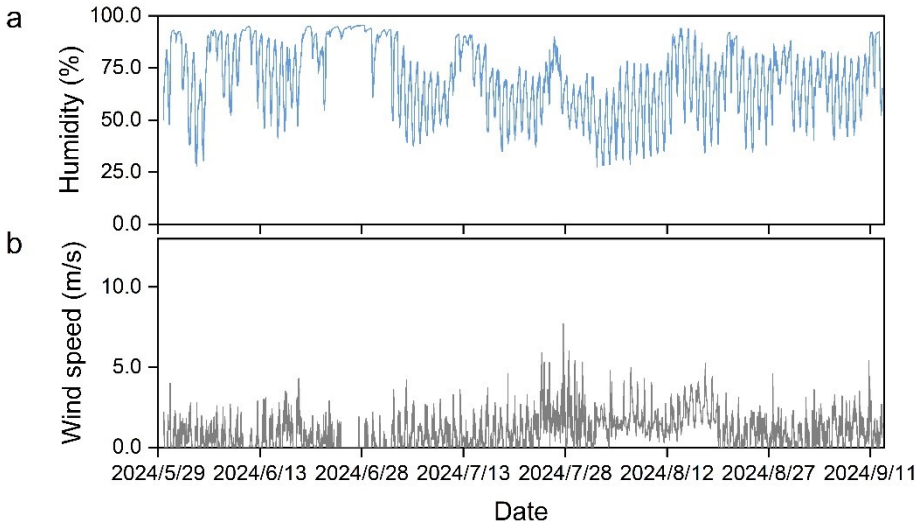

Fig S8. Local meteorological data (a) Humidity; (b) Wind speed.

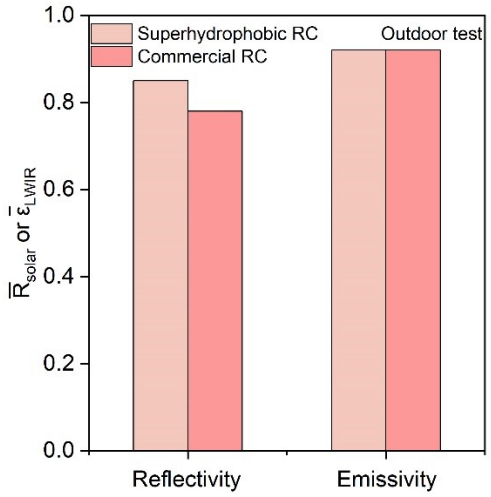

Fig S9. Comparison of reflectivity and emissivity between commercial RC and superhydrophobic RC after outdoor testing.

S5 Acid resistance test

Given the prevalence of acid rain deposition in mainland China (with a pH range of 4.34-5.6)[1], we conducted a systematic evaluation of the acid resistance of commercial RC and superhydrophobic RC materials. To simulate realistic chemical exposure conditions, three sulfuric acid solutions with pH values of 4.0, 5.0, and 5.6 were prepared, corresponding to the lower, median, and upper threshold values of typical acid rain events. Samples were subjected to a 24-hour soaking at room temperature (25 ℃), and after 24 hours, remove the material and dry it in an oven.

As demonstrated in Fig S10a, the superhydrophobic RC exhibits outstanding acid resistance while maintaining its radiative functionality. After being immersed in pH=4 sulfuric acid solution for 24 hours, the superhydrophobic RC showed a reflectivity of 0.89 and an emissivity of 0.93, comparable to the values of commercial RC. This significant stability indicates that the acid environment does not degrade the performance of the superhydrophobic coating.

We assessed the self-cleaning performance of the superhydrophobic RC after 24 hours of immersion in different acidic solutions and found that even under pH=4 conditions, the superhydrophobic RC maintained a CA of 145.8° and a SA of 6.2°, demonstrating good superhydrophobic properties. As shown in Fig S10d, under the extreme conditions of pH=4, the surface of the superhydrophobic RC remained free of noticeable cracks, with the microstructure still exhibiting a micro/nano structured layering, and the surface roughness maintained at a high level of 32.01 μm.

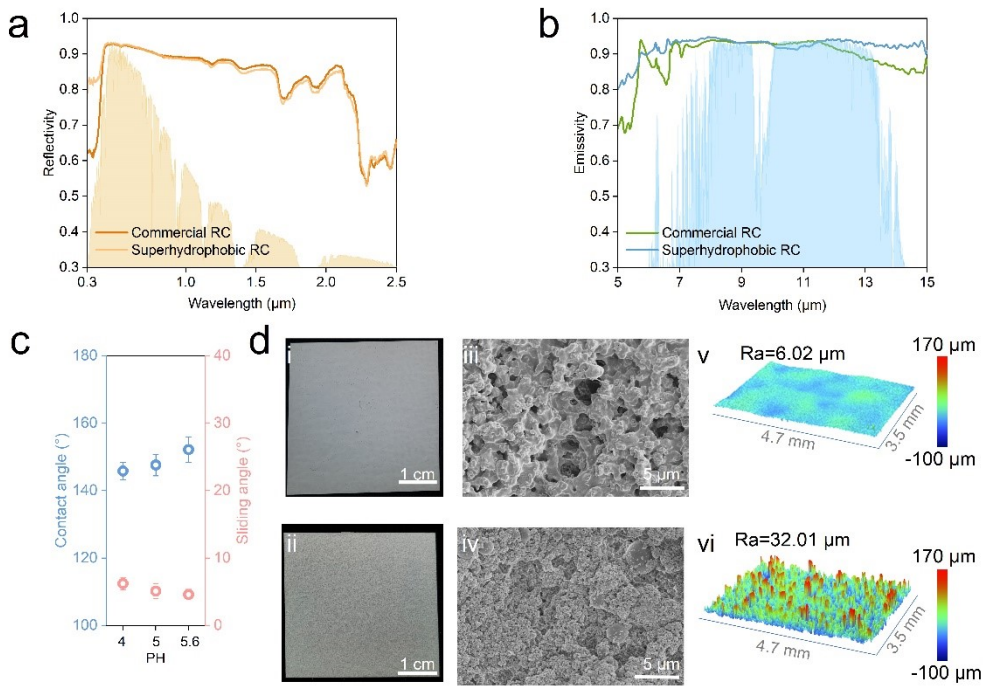

Fig S10. Anti-aging performance under acid resistance testing: (a) Reflectivity after acid resistance testing at pH=4; (b) Emissivity after acid resistance testing at pH=4; (c) Values of CA and SA for superhydrophobic RC during acid resistance testing; (d) Appearance, microstructure, and surface roughness after acid resistance testing at pH=4.

S6 Aging test

Rain resistance durability test. The rain resistance test of the samples was assessed by subjecting the samples to continuous rinsing with simulated rainfall at a rate of 133.33 mm/h for 48 hours (The total was 6400 mm). Based on the 2022 annual average rainfall of 1500.6 mm at the experimental location (Hangzhou), this is equivalent to 4.3 years of rainfall. The CAs and SAs were measured after drying in an oven. Table S1 shows the 2022 annual rainfall of selected provincial capital cities in mainland China (The simulated rainfall corresponds to the equivalent of n years under natural conditions).

Table S1. Rainfall of selected provincial capital cities/municipalities directly under the central government in mainland China for 2022

City	Rainfall (mm)	*n*
Shenyang	1039.7	6.2
Changchun	732.5	8.7
Haerbin	552.9	11.6
Beijing	585.4	10.9
Tianjin	618.2	10.4
Shijiazhuang	446	14.3
Taiyuan	502.3	12.7
Jinan	906.8	7.1
Shanghai	1044.1	6.1

Nanjing	819.8	7.8
Hangzhou	1500.6	4.3
Hefei	805.6	7.9
Fuzhou	1318.7	4.9
Nanchang	1559.1	4.1
Zhengzhou	470.6	13.6
Wuhan	1250.7	5.1
Changsha	1338.2	4.8
Chongqing	1082.4	5.9
Chengdu	983.1	6.5
Guangzhou	1959.8	3.3
Nanning	1105.9	5.8
Haikou	2020.9	3.2
Guiyang	1056.5	6.1
Kunming	1033.2	6.2
Xian	571.8	11.2
Lanzhou	195.1	32.8
Xining	515.4	12.4
Yingchuan	259.9	24.6
Urumqi	204.6	31.3
Lhasa	273.5	23.4

Soiling test. The soiling test involved spraying soiling agents onto the surface of the samples until different amounts of soiling agents accumulate per square centimeter of the surface. The samples were then dried in an oven. The soiling agent was prepared according to the standard ASTM D7897-18. The components are as follows:

(1) Dust: A mixture consisting of 0.3 ± 0.02 g of Fe_2O_3, 1.0 ± 0.05 g of montmorillonite, and 1.0 ± 0.05 g of bentonite was added to 1 L of distilled water to prepare a suspension and the final concentration was 2.3 ± 0.1 g/L.

(2) Salt solution: A mixture of 0.3 ± 0.03 g of NaCl, 0.3 ± 0.03 g of $NaNO_3$, and 0.4 ± 0.03 g of $CaSO_4 \cdot 2H_2O$ was dissolved in 1 L of distilled water to prepare a solution and the final concentration of 1.0 ± 0.1 g/L.

(3) Soot: A total of 0.26 ± 0.01 g of carbon black was dissolved in 1 L of distilled water to prepare the suspension.

Soiling agent mass was 79 % dust, 20 % salt solution and 1 % soot.

Ultraviolet (UV) durability test. The UV test involves exposing the sample to UV light for 42 days (0.89 W/m², center wavelength 340 nm, 60 °C), which is equivalent to 1 year of natural sunshine in Florida (annual UV dosage of about 275 MJ/m^2)[2].

S7 Area of different types of building stock in mainland China

The estimation of the floor area of different types of building stocks in this study is based on data from the "China Population Census Yearbook 2020" published by the National Bureau of Statistics in 2020 and the "China Building Industry Yearbook" issued by the China Construction Industry Association from 2001 to 2020. The specific calculation method is as follows: The current residential building stock area for each province is computed using the population numbers and per capita housing area of mainland China provinces as listed in the "China Population Census Yearbook" (Table S2). Subsequently, the floor area of different types of buildings completed between 2001 and 2020 is calculated using the data from the "China Construction Industry Statistical Yearbook," to determine the proportion of completed floor area by building type (Table S3). The floor area of various types of building stocks in each province (Fig S11) is then determined based on these calculations of residential building stock area and the proportions of various types of completed buildings.

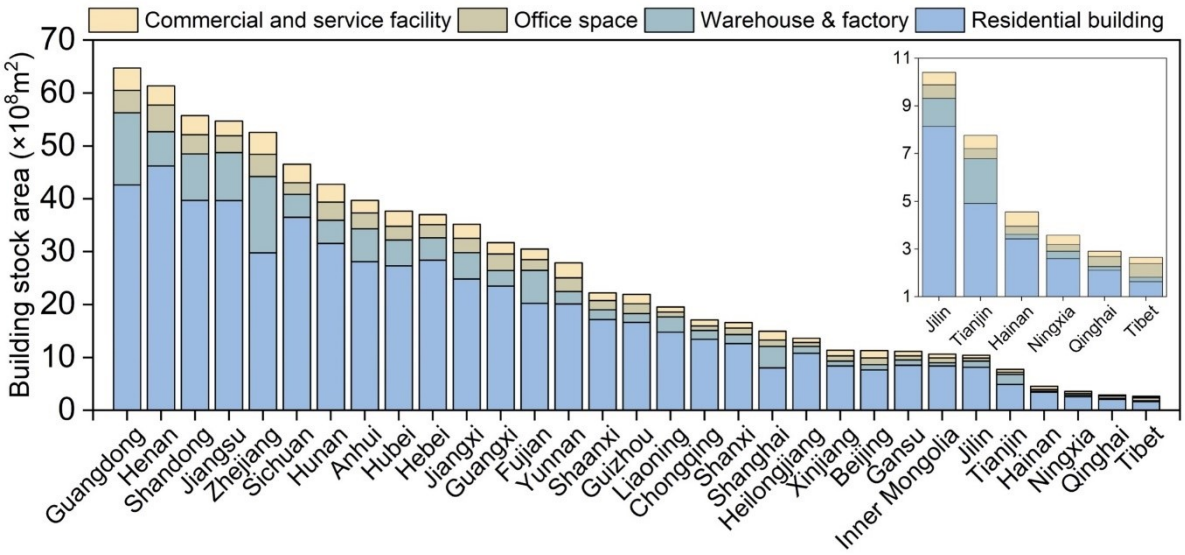

Fig S11. Floor area of different types of building stocks in each province/autonomous region/ municipality directly under the central government as of 2020.

Table S2. Population numbers and per capita housing area for each province/municipality directly under the central government

Province	Population Size (People)	Per capita housing area (m^2)
Beijing	21893095	34.89
Tianjin	13866009	35.45
Hebei	74610235	38.08
Shanxi	34915616	36.16
Inner Mongolia	24049155	34.96
Liaoning	42591407	34.70
Jilin	24073453	33.84
Heilongjiang	31850088	33.95
Shanghai	24870895	32.28
Jiangsu	84748016	46.80
Zhejiang	64567588	46.16
Anhui	61027171	46.08
Fujian	41540086	48.72
Jiangxi	45188635	54.96
Shandong	101527453	39.13
Henan	99365519	46.50
Hubei	57752557	47.31
Hunan	66444864	47.52
Guangdong	126012510	33.84

Guangxi	50126804	46.88
Hainan	10081232	33.98
Chongqing	32054159	41.96
Sichuan	83674866	43.63
Guizhou	38562148	43.10
Yunnan	47209277	42.61
Tibet	3648100	44.88
Shaanxi	39528999	43.44
Gansu	25019831	34.15
Qinghai	5923957	35.61
Ningxia	7202654	36.10
Xinjiang	25852345	32.52

Table S3. Proportional floor area of different types of building stocks in each province/municipality directly under the central government

Province	Residential building	Commercial and service facility	Office space	Warehouse & factory
Beijing	0.6042	0.1077	0.1019	0.0797
Tianjin	0.5534	0.0622	0.0472	0.2113
Hebei	0.6974	0.0469	0.0605	0.1041
Shanxi	0.6745	0.0553	0.0669	0.0912
Inner Mongolia	0.7081	0.0606	0.0762	0.0507
Liaoning	0.7087	0.0451	0.0444	0.1388
Jilin	0.7210	0.0458	0.0506	0.1036
Heilongjiang	0.7180	0.0545	0.0508	0.0844
Shanghai	0.4879	0.1023	0.0735	0.2457
Jiangsu	0.6807	0.0476	0.0543	0.1561
Zhejiang	0.5265	0.0739	0.0742	0.2545
Anhui	0.6457	0.0548	0.0685	0.1425
Fujian	0.6232	0.0619	0.0627	0.1920
Jiangxi	0.6382	0.0685	0.0701	0.1279
Shandong	0.6587	0.0597	0.0605	0.1451
Henan	0.6804	0.0532	0.0745	0.0953
Hubei	0.6619	0.0696	0.0633	0.1182
Hunan	0.6607	0.0709	0.0718	0.0916

Guangdong	0.5968	0.0592	0.0592	0.1910
Guangxi	0.6227	0.0562	0.0832	0.0778
Hainan	0.6143	0.1080	0.0614	0.0342
Chongqing	0.7282	0.0607	0.0460	0.0901
Sichuan	0.7177	0.0685	0.0432	0.0852
Guizhou	0.6270	0.0669	0.0697	0.0634
Yunnan	0.6105	0.0860	0.0789	0.0714
Tibet	0.5159	0.0821	0.1783	0.0586
Shaanxi	0.6911	0.0598	0.0690	0.0750
Gansu	0.6667	0.0660	0.0614	0.0776
Qinghai	0.5998	0.0622	0.1205	0.0446
Ningxia	0.6221	0.0936	0.0668	0.0747
Xinjiang	0.6306	0.0804	0.0747	0.0686

S8 Building energy simulation

EnergyPlus is a well-known comprehensive building energy analysis software that can analyze the year-round air conditioning energy consumption for various types of buildings. In mainland China, different types of buildings in different regions adhere to varying building standards, as detailed in Table S4. These standards, particularly those relating to external walls, roofing insulation layers, and the solar heat gain coefficients of windows, significantly influence the cooling energy consumption of buildings. To obtain realistic simulation data on cooling energy consumption that aligns with the actual conditions in mainland China, modifications were made to the building models' external walls, roofs, windows, and other relevant parameters based on regional standards. This adaptation ensures that the study's findings are applicable to the diverse climatic and regulatory environments across the country.

In the simulations conducted for this study, typical buildings of various architectural types were used. We assumed that commercial RC and superhydrophobic RC were applied to the rooftops of these typical buildings. The optical properties parameters for the outer surface materials of the rooftops incorporated are those of commercial RC and superhydrophobic RC after contamination with 8 mg/cm^2, including reflectivity in the 0.3-2.5 μm wavelength range and emissivity in the >2.5 μm range. This assumption was made to model the cooling energy consumption of different types of buildings after 3 years of dust contamination under natural conditions, and to

calculate the energy savings of buildings using superhydrophobic RC as compared to commercial RC.

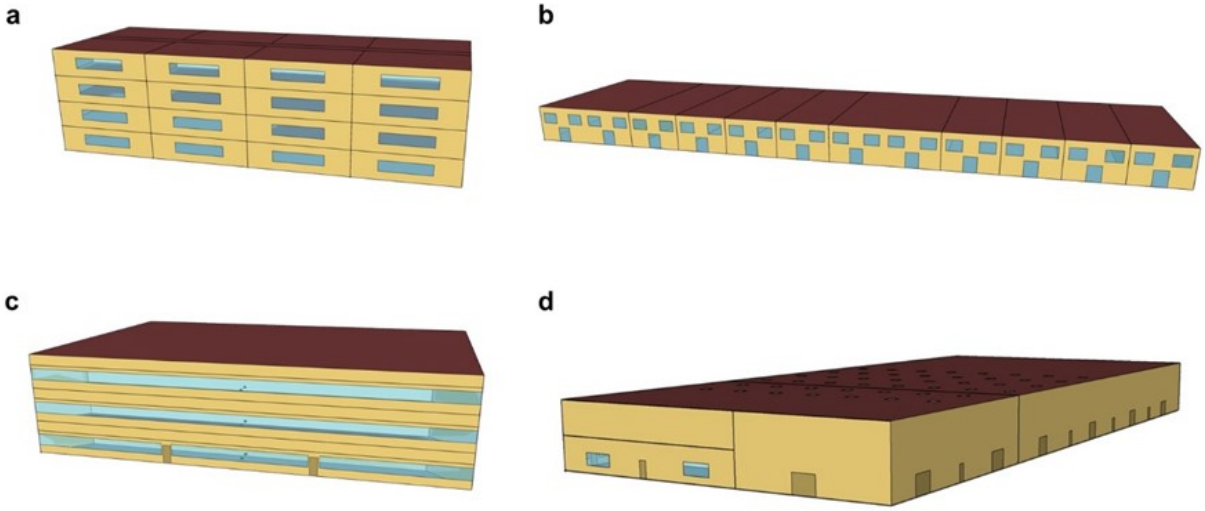

Fig S12. Typical building model (a) Residential building (b) Commercial and service facility (c) Office space (d) Warehouse & factory.

Table S4 The standards that apply to different building types

Building type	Comply with standards
Residential building	JGJ 134-2010
	JGJ 475-2019
	JGJ 26-2018
	JGJ 75-2012
Commercial and service facility	GB 50189-2015
Office space	GB 50189-2015
Warehouse & factory	GB 51245-2017

S9 Carbon emission factors by province in mainland China

In China, the power grid is categorized by size into the national grid, regional grids, and provincial grids. The smaller the scale of the grid, the more closely its emission factor approaches the actual indirect emissions per unit of electricity consumption. Therefore, in this study, to calculate the carbon emissions reduction of superhydrophobic RC houses compared to houses with commercial RC materials after pollution (the pollution level was 8 mg/cm²), we used the provincial-level electricity carbon emission factors from Mainland China for the year 2020[3]. The specific data can be found in Table S5.

Table S5. Provincial grid emission factors in mainland China for the year of 2020 ($kgCO_2/kWh$)[3]

Province	Carbom emission factor ($kgCO_2/kWh$)
Liaoning	0.91
Jilin	0.839
Heilongjiang	0.814
Beijing	0.615
Tianjin	0.841
Hebei	1.092
Shanxi	0.841
Inner Mongolia	1.000
Shandong	0.742
Shanghai	0.548
Jiangsu	0.695
Zhejiang	0.532
Anhui	0.763
Fujian	0.489
Jiangxi	0.616
Henan	0.738
Hubei	0.316
Hunan	0.487
Chongqing	0.432

Sichuan	0.117
Guangdong	0.445
Guangxi	0.526
Hainan	0.459
Guizhou	0.42
Yunnan	0.146
Shaanxi	0.641
Gansu	0.46
Qinghai	0.095
Ningxia	0.872
Xinjiang	0.749
Tibet	——

S10 Cost Analysis of the Superhydrophobic Coating

In consideration of the practical application potential of the proposed superhydrophobic coating, especially for large-scale industrial use, a preliminary cost analysis was conducted based on laboratory-scale conditions. The prices of the raw materials used in this study were obtained from the Zhejiang University Chemical Reagent Procurement and Management Platform. All USD prices were converted based on the exchange rate on June 4, 2025 (1 USD ≈ 7.2 CNY). The materials and their corresponding costs are as follows:

1. EA: \$16.49 USD / 2.5 L
2. n-SiO_2: \$20.78 USD / 500 g
3. μ-SiO_2: \$42.43 USD / 500 g
4. EP: \$80.00 USD / 500 g
5. PDMS (prepolymer + curing agent): \$90.28 USD / 550 g (500 g prepolymer + 50 g curing agent)

The calculated material cost is approximately \$21.02 USD/m² under laboratory-scale conditions. It should be noted that this cost reflects the use of small-batch, high-purity materials under research settings. In industrial-scale production, bulk purchasing and process optimization are expected to significantly reduce the overall cost.

For reference, the commercial RC substrate used in this study has a market price of approximately \$71.22 USD/m². Therefore, the added cost of the superhydrophobic

coating represents only a small proportion of the total system cost, highlighting its cost-effectiveness and potential for large-scale application.

References

[1] Chen X , Shan X, Shi Z, Zhang J, Zhong Q, Xiang H, Wei H, Analysis of the spatio-temporal changes in acid rain and their causes in China (1998–2018). *Journal of Resources & Ecology*. 2021, 12, 5.

[2] Song J, Zhang W, Sun Z, Pan M, Tian F, Li X, Ye M, Deng X, Durable radiative cooling against environmental aging. *Nature Communications.* **2022**, 13, 4805.

[3] China regional power grids carbon dioxide emission factors, 2023. https://www.caep.org.cn/sy/tdftzhyjzx/zxdt/202310/t20231027_1044179.shtml.